

## MICROSTRUCTURAL INVESTIGATIONS ON CATHODE/ELECTROLYTE SUPPORT USED FOR INTERMEDIAR TEMPERATURE SOLID FUEL CELL

Ionel MERCIONIU<sup>1</sup>,

*Lucrarea prezintă investigații microstructurale în sistemul catod-strat subțire/ electrolit solid preparat prin sinterizare utilizat în pilele de combustie de temperatură medie cu electrolit solid de medie temperatură (IT – SOFC). Au fost utilizate tehniciile: spectroscopie de difracție de raze X, microscopie electronică prin transmisie și microscopie electronică de baleaj.*

*This paper presents a microstructural investigation of the system cathode – thin layer / solid electrolyte – sintered body used for intermediate temperature solid oxide fuel cell (IT – SOFC). X-ray diffraction spectroscopy, transmission electron microscopy and scanning electron microscopy were used.*

**Keywords:** intermediate temperature solid oxide fuel cell (IT-SOFC), thin films, ceria, yttria

### 1. Introduction

Ceria-doped yttria has a fluorite type structure with enriched oxygen vacancies introduced by substituting trivalent Yttrium ( $Y^{3+}$ ) for quadrivalent Cerium ( $Ce^{4+}$ ). When 10 mol %  $Y_2O_3$  is substituted for  $CeO_2$ , the ionic conductivity of  $Y_2O_3$ -doped  $CeO_2$  at 1000 °C is  $\sim 0,15 \Omega cm^{-1}$ . At such a high ionic conductivity, the generation of oxygen site vacancies within the fluorite-type lattice may lead to interactions forming more ordered structures[1]. Ceria-doped yttria solid electrolytes are of a great interest for intermediate temperature solid electrolyte oxide fuel cells (IT SOFC) applications.

Reduction in the operating temperature of solid oxide fuel cells (SOFCs) to 700 – 800 °C requires the development of new cathode electrodes (films deposited on  $10Y_2O_3:CeO_2$  electrolyte-support) with high electrocatalytic activity for oxygen reduction. Promising alternative cathode materials are composites made of a perovskite with a solid electrolyte, e.g.  $La_{1-x-y}Sr_xMnO_{3-\delta}$  –  $ZrO_2(Y_2O_3)$ [2], which behave effectively as mixed conductors on the macroscopic scale. Besides their high oxygen ion conductivity, these materials are endowed

<sup>1</sup> PhD student, Department of Electrical Engineering, University POLITEHNICA of Bucharest, and Research Assist, National Institute of R&D for Materials Physics, Magurele, Romania, e-mail: ionel\_mercioniu@yahoo.com

with a high electronic conductivity leading to enlargement of the available surface area for oxygen reduction [3, 4]. The electrochemical performance of the studied materials is measured based on parameters such as: current density (voltage curves of single cells where the same anode is used)[4], individual polarization and impedance characteristics of the SOFC cathodes.

The present study performs a complete microstructural characterization of the system LSFC (La<sub>0.6</sub>Sr<sub>0.4</sub>Fe<sub>0.8</sub>Co<sub>0.2</sub>O<sub>3-δ</sub>)/CeO<sub>2</sub> (10 mol% Y<sub>2</sub>O<sub>3</sub>) system through analytical tools such as Transmission electron microscopy (TEM + SAED), X-Ray Diffraction (XRD) and (Scanning Electron Microscopy) SEM measurements.

## 2. Experimental

Fine Ce-Y oxide nanopowders represent the starting materials. The coprecipitation method was used to prepare the specimens for further analysis as it was previously reported [8, 9] to yield a thoroughly blended powder, thus eliminating errors in the measurements.

### 2.1 (10 mol %) Y<sub>2</sub>O<sub>3</sub> doped CeO<sub>2</sub>, nanopowders

To obtain CeO<sub>2</sub> + 10 mol%Y<sub>2</sub>O<sub>3</sub> as solid electrolyte, Ce(NO<sub>3</sub>)<sub>3</sub>·6H<sub>2</sub>O crystals of Ce(NO<sub>3</sub>)<sub>3</sub>·6H<sub>2</sub>O, Y<sub>2</sub>O<sub>3</sub> nanopowder, distilled water and NH<sub>4</sub>NO<sub>3</sub> were mixed together[8, 9]. The preparation of the sample took place in several stages: i) the preparation of a suspension by dispersing Y<sub>2</sub>O<sub>3</sub> nanopowder in distilled water; ii) preparation of Ce(NO<sub>3</sub>)<sub>3</sub>·6H<sub>2</sub>O solution in distilled water (50%); iii) mixing the Y<sub>2</sub>O<sub>3</sub> suspension with Ce(NO<sub>3</sub>)<sub>3</sub>·6H<sub>2</sub>O solution by using a magnetic agitator; iv) addition (through dropping) of NH<sub>4</sub>NO<sub>3</sub> aqueous solution (50% volume)–in excess; v) agitation for 3 hours (by means of an magnetic agitator) of the final mixture, to complete the oxide-reduction reaction; vi) filtration under vacuum resulting in a final co-precipitate product; vii) washing the final co-precipitate product with distilled water followed by washing in ethanol to remove the water traces; viii) drying the final product in a muffle furnace for 24 h, to remove the alcohol; ix) grinding and sieving; x) calcinations for 2h at T=500 °C to obtain a nanopowder. Further on, the nanopowders were isostatic compressed at 200 MPa to obtain the 10Y<sub>2</sub>O<sub>3</sub>:CeO<sub>2</sub> green body. The resulted green bodies were sintered at 1400 °C, 1450 °C, 1500 °C and 1550 °C for 2 h.

The resulted nanopowder was further analysed by X-ray Diffraction (XRD) and Transmission Electron Microscopy (TEM) and the green body and sintering body were analysed by X Ray Diffraction (XRD) and (Scanning Electron Microscopy) SEM [10].

## 2.2 Pulse laser ablation for deposition the cathode film

The  $\text{La}_{0.6}\text{Sr}_{0.4}\text{Fe}_{0.8}\text{Co}_{0.2}\text{O}_{3-\delta}$  (LSFC) cathode was obtained by Pulse Laser Ablation (PLA). PLA is a deposition method of nano or micro layers of material starting from a bulk target that is melted and vaporized under the action of multipulse laser pulse irradiation [5]. Due to the high intensity of the pulse correlated to the short duration, the material residing on the surface of the target surface is transformed in ionized gas characterized by highly energetic species. In a subsequent step a liquid component made of nanoparticles is expulsed from the target [6]. Thus, the pulsed laser beam is employed to ablate a target composed of the desired film material, which is subsequently deposited onto the Ce-Y electrolyte substrate. The PLA experiments were performed, using a KrF excimer laser source ( $\lambda=248$  nm,  $\tau=25$  ns), a laser energy of 450 mJ, a laser fluence (energy/surface) set at  $3\text{J/cm}^2$ , at a support temperature  $200\text{ }^{\circ}\text{C}$ .

The structure of the resulting cathode/electrolyte system specimens was investigated by: X-ray diffraction (XRD), transmission electron microscopy (TEM, SAED) and scanning electron microscopy (SEM), in correlation with statistical measurements [7].

XRD spectrum has been obtained using a Bruker D8 Advance diffractometer with  $\text{CuK}\alpha$  source cathode.

The conventional transmission electron microscopy (TEM) was performed on a JEOL 200CX electron microscope and the scanning electron microscopy was performed on a Hitachi S2600N device.

## 3. Results and discussions

The obtained XRD spectrum of the PLA deposited LSFC ( $\text{La}_{0.6}\text{Sr}_{0.4}\text{Co}_{0.2}\text{Fe}_{0.8}\text{O}_{3-\delta}$ ) on Ce-Y (sintered body) electrolyte is shown in Fig. 1. The diffraction lines of LSFC rhombohedral phase [ASTM 00-049-0284] are clearly seen, while the diffraction lines of  $\text{CeO}_2$  cubic phase [ASTM: 03-065-5923], with the unit cell parameter appears to be slightly modified [ $a(\text{CeO}_2)=5.404\text{ \AA}$ ;  $a(\text{Ce-Y})=5.392\text{ \AA}$ ]. Such a change might have occurred due to the presence of yttria in the ceria structure. This information proves the achievement of the optimum laboratory procedures, to obtain the cathode/electrolyte (LSFC/Ce-Y) systems.

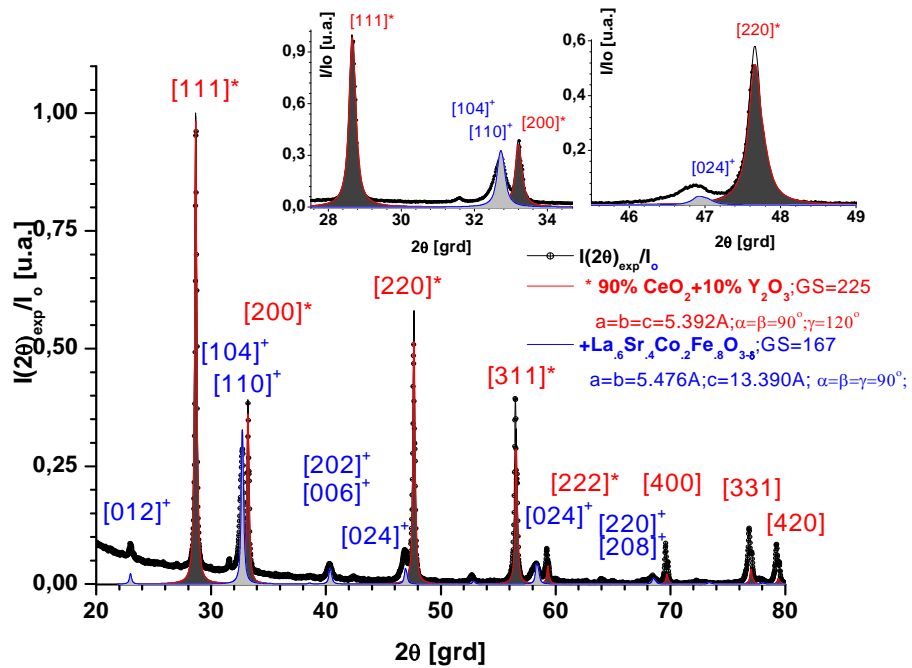


Fig.1. The XRD spectrum of the PLA deposited LSFC ( $\text{La}_{0.6}\text{Sr}_{0.4}\text{Co}_{0.2}\text{Fe}_{0.8}\text{O}_{3-\delta}$ )/Ce-Y cathode nanopowder

The results of transmission electron microscopy (TEM) and selected area electron diffraction (SAED) on: (a) electrolyte nanopowders obtained by co-precipitation and calcined at  $500^{\circ}\text{C}$ , and (b)  $\text{La}_{0.6}\text{Sr}_{0.4}\text{Fe}_{0.8}\text{Co}_{0.2}\text{O}_{3-\delta}$  (LSFC) cathode nanopowder (INFRAMAT) are presented in the Figs. 2 and Figs. 3, respectively, as well as the shape and distribution of the particles, the main dimensional value of the particles and the defects, the porosity in particle and in agglomerates.

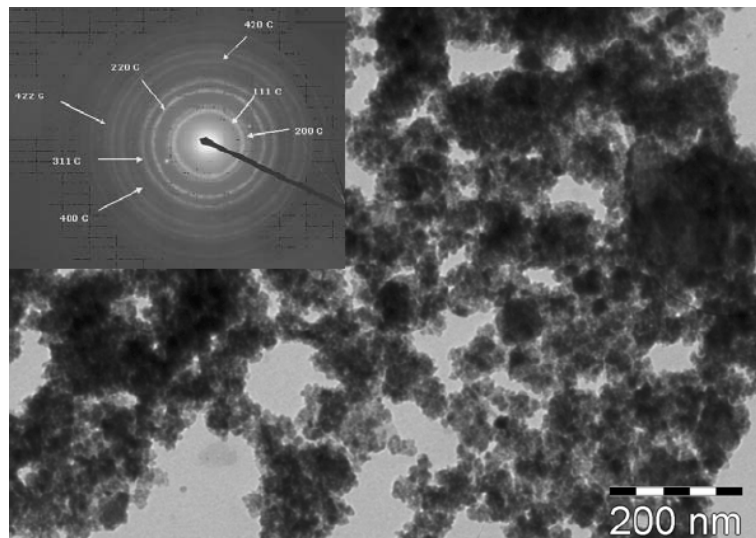


Fig. 2. TEM and SAED images of  $\text{Y}_2\text{O}_3$ :  $\text{CeO}_2$  nanopowders [ASTM: 03-065-5923]

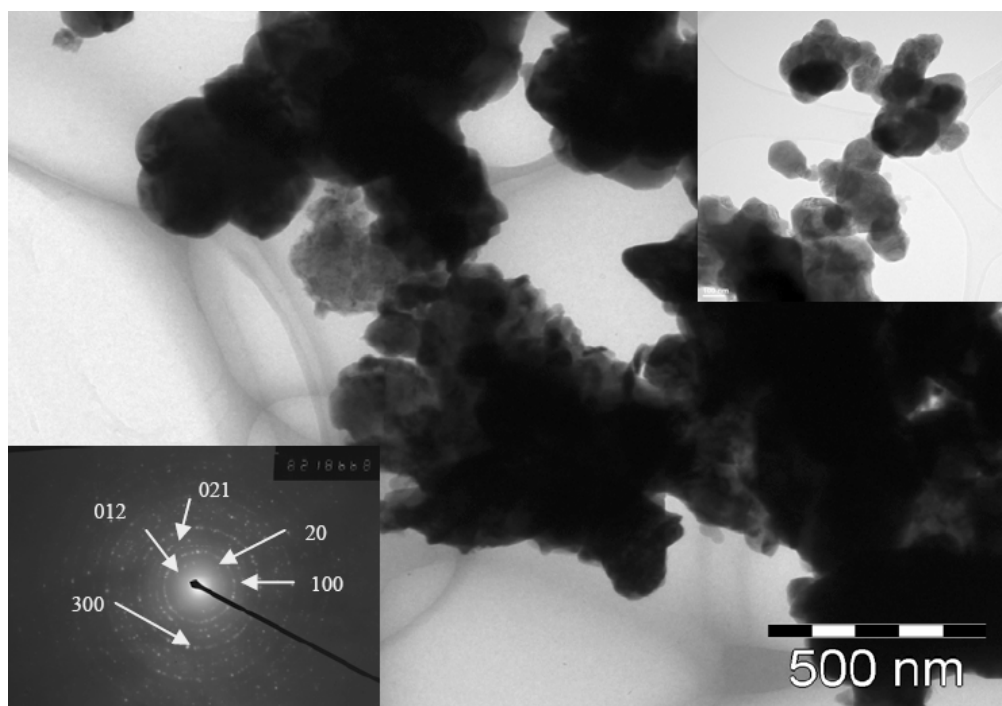


Fig. 3. TEM and SAED images of  $\text{La}_{0.6}\text{Sr}_{0.4}\text{Fe}_{0.8}\text{Co}_{0.2}\text{O}_{3-\delta}$  nanopowders [ASTM: 48-0125]

The interpretations of TEM+SAED results, in correlation with statistical measurements, obtained on minimum 100 images, for both powders [electrolyte and cathode] are presented in Table 1.

*Table 1*  
**Morphological data of transmission electron microscopy in correlation with statistical determination**

Nanopowders samples	Shape of particles	Interval of dimensional variations [nm]	Mean value of particles diameter [nm]	Observations
10Y <sub>2</sub> O <sub>3</sub> : CeO <sub>2</sub>	Uniform and crystalline spherical nanoparticles, with a good statistical dimensional repartition: the standard deviation is small.	5.88–15.15	8.112±0.052	Particles are not porous, porosity is present agglomerates
La <sub>0.6</sub> Sr <sub>0.4</sub> Fe <sub>0.8</sub> Co <sub>0.2</sub> O <sub>3-δ</sub> LSFC	Uniform and crystalline spherical nanoparticles, with a good statistical dimensional repartition; the presence of a system of agglomerates with the mean dimensional values around 140 nm	20.8–118	58.2 ±0.982	Particles are not porous, but it is a porosity in agglomerates (practically between nano particles)

Qualitative and quantitative analysis of the sample morphology was considered using a Hitachi S2600N microscope SEM equipped with an EDX (energy dispersive X-ray) detector. A thin film of copper coated the samples prior to SEM investigations. Table 2, Figs. 4 and 5 reveals the findings of the.

*Table 2*  
**Results of SEM/EDX**

Sintering bodies samples	Shape of grains	Interval of dimensional variation [μm]	Mean value of grains diameter [μm]	Observations
10Y <sub>2</sub> O <sub>3</sub> : CeO <sub>2</sub>	Polyhedral grains with rounded edges	0.82 – 2.85	1.342 ± 0.185	Low porosity
La <sub>0.6</sub> Sr <sub>0.4</sub> Fe <sub>0.8</sub> Co <sub>0.2</sub> O <sub>3-δ</sub>	Spherical grains	0.5 – 5.6	2.18 ± 0.074	Porosity ~ 32%

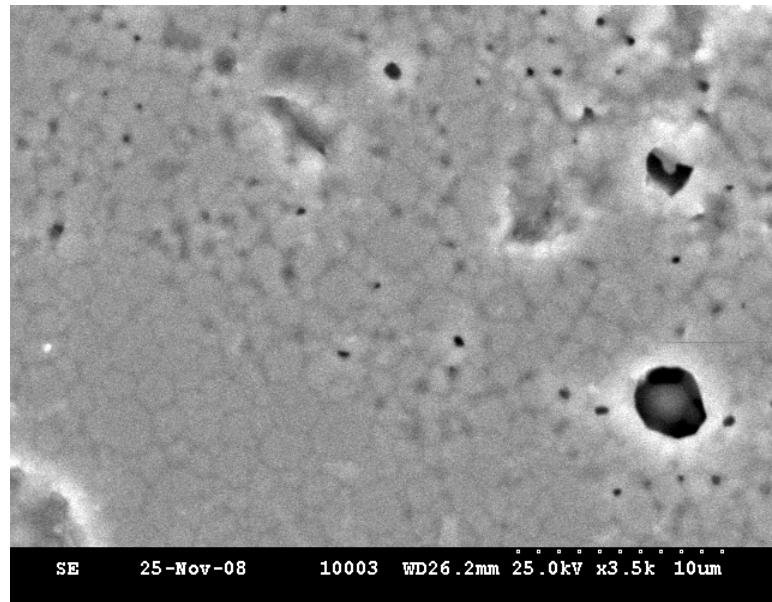


Fig. 4a. SEM on 10Y<sub>2</sub>O<sub>3</sub>: CeO<sub>2</sub> electrolyte

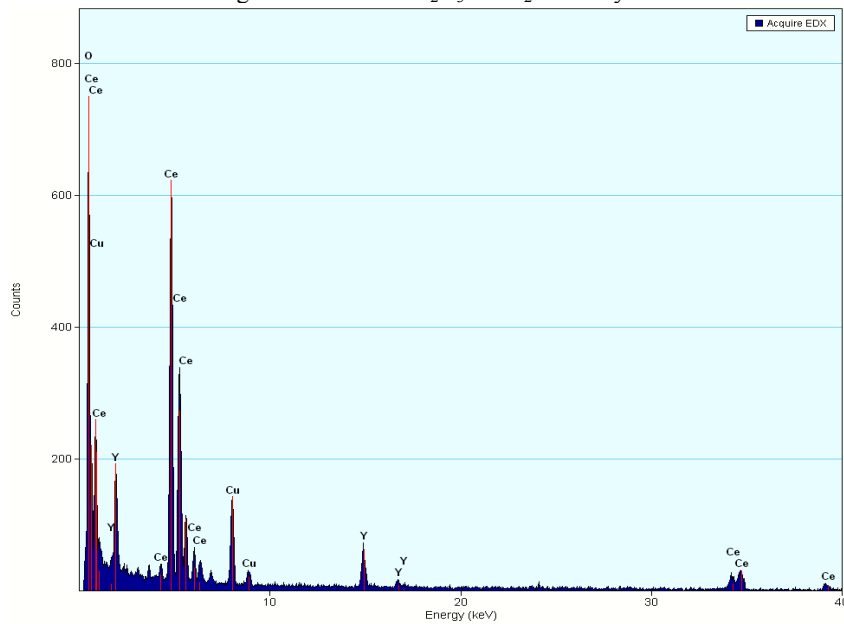


Fig. 4b. EDX spectrum of 10Y<sub>2</sub>O<sub>3</sub>: CeO<sub>2</sub> electrolyte

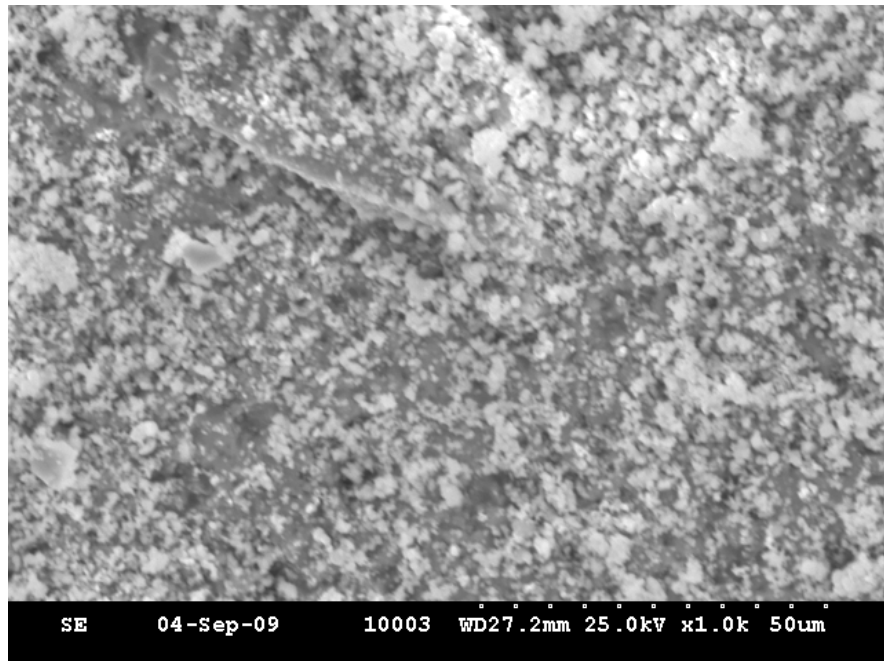


Fig.5a. SEM micrograph of  $\text{La}_{0.6}\text{Sr}_{0.4}\text{Fe}_{0.8}\text{Co}_{0.2}\text{O}_{3-\delta}$  cathode

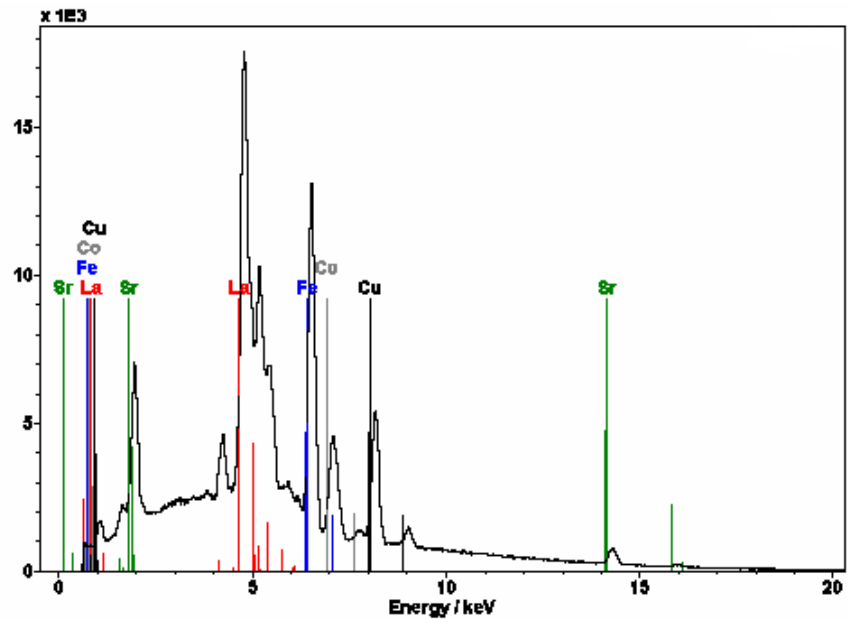


Fig.5b. EDX spectrum of  $\text{La}_{0.6}\text{Sr}_{0.4}\text{Fe}_{0.8}\text{Co}_{0.2}\text{O}_{3-\delta}$  cathode

The TEM and SAED investigations on the nanopowders (electrolyte and cathode) samples (Figs. 2, 3) show the following:

- (a) **cathode:** • the powder is crystalline and uniform • the shape of the nanoparticles is spherical, with a normal dimensional repartition; • the powder contains agglomerates with a mean dimensional values around 140 nm; • the mean value of the particles is  $(58.2 \pm 0.982)$  nm; • the porosity is around 32% • the mean pore size is  $(0.2 \pm 0.09)$   $\mu\text{m}$ ;
- (b) **electrolyte:** the powder is crystalline and uniform; • the shape of particles is spherical, with a normal dimensional repartition • the standard deviation around the mean size value of the particles distribution is small; • the mean particle size is  $(8.112 \pm 0.052)$   $\mu\text{m}$ .

The SEM and EDX investigations on cathode-layers /electrolyte as sintered bodies (Figs. 4 and 5) show the following aspects:

- ❖  $\text{La}_{0.6}\text{Sr}_{0.4}\text{Fe}_{0.8}\text{Co}_{0.2}\text{O}_{3-\delta}$  - cathode film has spherical grains with a mean dimensional value  $(2.18 \pm 0.074)$   $\mu\text{m}$ ; the porosity is around 32 %;
- ❖  $10\text{Y}_2\text{O}_3$ :  $\text{CeO}_2$  – electrolyte (sintered body) has polyhedral grains with rounded edges with a mean dimensional value  $(1.342 \pm 0.185)$   $\mu\text{m}$ ; the porosity is low.

#### 4. Conclusions

The complete microstructural analysis of the cathode/electrolyte system considered in the previously study revealed the followings aspects:

- the microstructure of the cathode (film) in correlation with the microstructure of the electrolyte (sintering body) showed a good compatibility and evidenced the interface in which one observes the interdependence between the both phases;
- the porosity of the cathode was found to be around 32% while the porosity of the electrolyte foretell was < 2 % allowing a good functionality of the IT-SOFC system;
- the repartitions of the particles (for powders) and of the grains (for film and sintering body) were found to be in a normal range good accordance with the microstructure;
- the EDX spectra showed a good delimitation between the cathode and electrolyte.

#### Acknowledgment

The author thanks Dr. P. Nita for the SEM images and the EDX spectra and prof. P. Notinger for the long and fruitful discussions.

The author thank gratefully acknowledge the financial support on the PN II 71-031/2007 project.

## R E F E R E N C E S

- [1] *A.L. Dragoo, L.P. Domingues*, "Preparation of High-Density Ceria- Yttria Ceramics", *J. Am. Ceram. Soc.*, **Vol. 65**, No. 5, (1982), pp. 253 – 259
- [2] *T. Kenjo, M. Nishiya*, "LaMnO<sub>3</sub> air cathodes containing ZrO<sub>2</sub> electrolyte for high temperature solid oxide fuel cells" *Solid State Ionics* 57 (1992) pp. 295 – 302
- [3] *A. Mai, V.A.C. Haanappel, S. Uhlenbruck, F. Tietz, D. Stöver*, "Ferrite-based perovskites as cathode materials for anode-supported solid oxide fuel cells", *Solid State Ionics* 176 (2005) 1341–1350
- [4] *S. Bebelis, N. Kotsionopoulos, A. Mai, D. Rutenbeck, F. Tietz*, "Electrochemical characterization of mixed conducting and composite SOFC cathodes", *Solid State Ionics* 177 (2006) 1843–1848
- [5] *R. Eason (Ed.)*, *Pulsed Laser Deposition of Thin Films: Applications-Led Growth of Functional Materials*, Wiley-Interscience, (2006)
- [6] *S.Noël, J.Hermann*, "Reducing nanoparticles in metal ablation plumes produced by two delayed short laser pulses" *Appl. Phys. Lett.*, 94, (2009), pp. 053120 -1 – 053120 – 3,
- [7] *C. Granqvist, L. Kish, W. Marlow (Eds)*, *Gas Phase Nanoparticle Synthesis*, Springer, (2005)
- [8] *N. Popescu – Pogriion et al*, *J. Am. Ceram. Soc.*, *in press*
- [9] *A. Moure, J. Tartaj, C. Moure*, "Synthesis and Low-Temperature Sintering of Gd-doped CeO<sub>2</sub> Ceramic Materials Obtained by a Coprecipitation Process", *J. Am. Ceram. Soc.*, 92 (10) (2009), pp. 2197–2203
- [10] *G. Veliciu, C. Seitan, F. Bogdan, G. Sbarcea*, "Materiale compozite folosite in calitate de anod pentru pilele SOFC", *RRM*, 3/2009, pag. 180–187.